Физика твердого тела, 2004, том 46, вып. 4

Electron emission properties of detonation nanodiamonds

© V.V. Zhirnov[*], O.A. Shenderova[*,**], D.L. Jaeger[*,**], T. Tyler[*], D.A. Areshkin[*], D.W. Brenner[*], J.J. Hren[*]

[*] North Carolina State University, Raleigh,
NC 27695-7907, USA
[**] International Technology Center, Research Triangle Park,
NC 27709, USA

This paper summarizes results of systematic studies of field electron emission from detonation nanodiamond coatings corresponding to nanodiamond powders of different modifications. The role of chemical composition of the surface of detonation nanodiamond particles in field emission mechanisms is discussed. Field emission related electronic properties of single diamond nanodots are studied using tight-binding calculations and continuum electrostatic simulations.

D.W.B., O.A.S. and D.A.A. acknowledge funding by the Office of Naval Research (Contract N 00014-95-1-0279), O.A.S. and D.L.J. — the Office of Naval Research (Contract N 00014-02-1-0711).

1. Introduction

Extensive studies of field electron emission from diamond have been carried out during the past several years (for a review see ref. [1]). It was observed experimentally that coating metal field emitters with diamond films (CVD, natural diamond, HPHT, etc.) could significantly enhance electron emission [1]. However, the mechanism of electron emission in such structures is not completely understood because they are complex. The properties of the surface (e. g. electron affinity), new interfaces (e. g. grain boundaries), material inhomogeneities, and/or doping can have dramatic effects on the emission behavior of these composite emitters.

Diamond nanodots (DND) produced by detonation are the smallest (2–5 nm in size) currently observed particles of diamond matter, with many properties still unknown. Deposition of the detonation DND on the top of field emission tips allows one to obtain information about electronic properties of DND from field emission experiments along with information about structure and composition from non-destructive high-resolution transmission electron microscopy.

2. Detonation Nanodiamond Coatings

Detonation DND were deposited onto sharp field emission tips (Si and Mo; curvature radius 10–100 nm) by pulsed electrophoresis, in a suspension of diamond nanoparticles in alcohol (for details see Refs. [2–4]). The resulting deposits of diamond nanoparticles were found to depend upon applied voltage, suspension concentration, pulse duration, and tip geometry. This procedure resulted in sufficient control to prepare metal needles with deposits varying from isolated diamond nanodots to continuous nanodiamond films of varying thickness.

Three different types of detonation diamond [5], shown in Table 1, were investigated. Detonation diamond nanoparticles were prepared in the Russian Federal Nuclear Center — All-Russian Institute of Technical Physics (VNIITF — Snezhinsk).

Emission $J-F$ (current density vs electric field) characteristics were measured. To compare different coatings of different type of nanodiamond, the two parameters were chosen: emission threshold field (F_{th}), and integral normalized transconductance ($g_n = \frac{1}{J}\frac{\Delta J}{\Delta F}$), which as is a measure of steepness of $J-F$ characteristics. As can be

Table 1. Properties of three types of detonation nanodiamond particles [5] and field electron emission parameters of corresponding nanodiamond coatings

Nanodiamond type	USDD2	USDD3	USDD4
Alternative name	Nd	NdP1	NdO
Description	standard	USDD2 with additional acid & high-temperature treatment	USDD3 with additional ozone treatment
Impurities	O,N,H ∼ 8–10%	O,N,H ∼ 2–4%	N,O ∼ 6%
pH of 10% water susp.	5.6–6.2	3.5–4.5	1.6–2.0
Field electron emission parameters			
Change in field emission threshold, compared to bare Si field emitter	−15%	−25%	−15%
Change in normalized integral transconductance, compared to bare Si field emitter	−37%	−30%	+33%

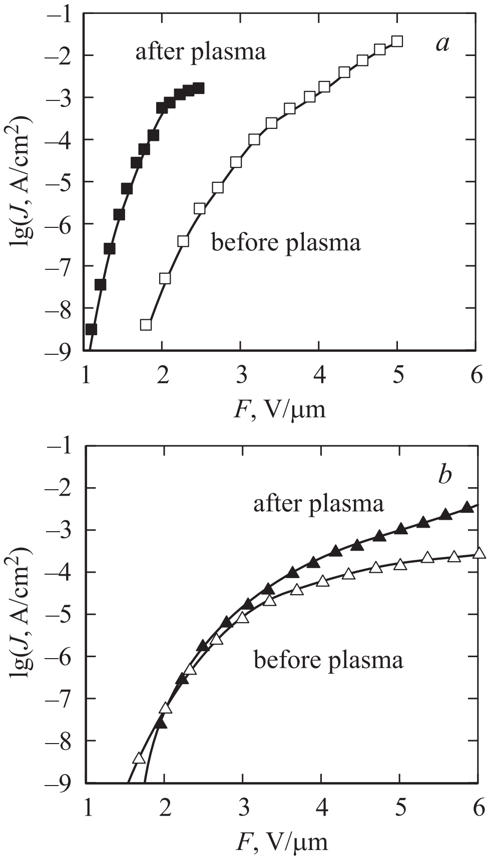

Figure 1. Hydrogen plasma effect on emission characteristics of detonation nanodiamond coatings: (*a*) NdO and (*b*) NdP1.

seen from Table 1, all three types of nanodiamond coatings showed an improvement in the emission threshold, the smallest threshold was observed for NdP1 coating. However, the effect of the coatings on the normalized integral transconductance (steepness) was different for different coatings. While the NdO coating resulted in much steeper $J-F$ characteristics, as compared to the bare Si emitter, emitters with detonation nanodiamond and NdP1 coatings showed very shallow characteristics in the higher current region (low transconductance). Additional hydrogen plasma treatment was used to modify surface properties of emitters with NdO and NdP1 coatings (for details see ref. [2]). Fig. 1 shows emission characteristics before and after the plasma treatment. As can be seen, the effects of hydrogen plasma are very different for the two types of nanodiamond.

For the NdO coating, emission threshold remarkably decreased after H-plasma, and $J-F$ characteristic shifted to the left. The emission threshold improvement was 35% relative to the NdO emitter before hydrogen plasma treatment and 45% relative to the bare Si field emitter. The hydrogenated NdO coating was found to be the best emissive coating in this series of experiments, with both lowest emission threshold and highest transconductance.

For the NdP1 coating (Fig. 1, *b*), the emission threshold did not change after treatment in hydrogen plasma. However, the high-current part in the emission characteristics shifted up, indicating an increase in transconductance.

The difference in emission properties of NdO and NdP1 nanodiamond coatings reflects the importance of surface modification. The emission results can be interpreted in terms of the two-barrier Metal–Diamond–Vacuum emission model. In this model, electrons are injected from the conductive electrode (e.g. field emission tip) into diamond through an interface barrier. Then the electrons move to the diamond-vacuum interface, and escape to vacuum through the surface barrier (e.g. the electron affinity). The transparency of both barriers determines the emission threshold. During electron transport in diamond, there are several physical phenomena resulting in the „resistance“ of the diamond film, such as negative and positive space charge effects, scattering, hopping conductance, etc. These „resistive“ effects limit the supply of electrons to the surface, which result in shallow or saturated current-voltage characteristics in the higher current region (e.g. lower transconductance).

Nanodiamond of NdO type was treated by ozone, and correspondingly, it contains larger amounts of oxygen on the surface. Oxygen, being an electronegative element, is known to increase electron affinity of diamond surface. Hydrogen plasma treatment replaces oxygen with hydrogen, which is known to decrease the electron affinity of diamond. Based on the Fowler–Nordheim equation for field emission, the shift of emission characteristics in Fig. 1, *a* corresponds to a decrease in the effective surface barrier of 0.9 eV.

Nanodiamond of NdP1 type (without ozone treatment) apparently contains smaller amounts of oxygen, but larger amounts of H and N atoms on the surface. Its emission threshold before H-plasma treatment is lower than NdO, however the transcondactance is lower, due to „resistive“ (e.g. negative shace charge) effects at higher currents. After H-plasma, the emission threshold did not change, however, the „resistance“ effects became smaller (the transconductance increased). This could indicate on a role of nitrogen in the resistance effects, since oxygen-rich samples did not show the resistance effects, and the hydrogen content after plasma treatment at the same conditions should be similar in both samples.

3. Field emission from a single nanodiamond particle

We attempted to reduce the possible variables by performing experiments with controlled deposits of nanodiamond particles (USDD4 — NdO type) with an individual size of about 5 nm. Both the geometry of the underlying metal surface and the diamond particle were observed with atomic resolution in a transmission electron microscope. In the experiments reported here, isolated diamond nanoparticles were deposited onto Mo tips (Fig. 2, *a*), characterized by field emission, and then the resulting data compared to that of the bare metal tip before deposition (of the same specimen). Next, thicker nanodiamond coating

Table 2. Geometrical and emission parameters of nanodiamond field emitters

	Characteristics	Bare Mo	Single particle	ND film
Geometrical	Metal tip radius	50 nm	50 nm	50 nm
	ND Thickness	0 nm	2.3 nm	20 nm
Field Emission	Threshold voltage	172 V	222 V	89 V
	Transconductance	7.63 nA/V	7.09 nA/V	16.4 nA/V
Fowler–Nordheim Analysis	Apparent work function	4.05 eV	5.57 eV	2.71 eV

was deposited onto the same tip with subsequent field emission measurements. The results of these experiments are summarized in Table 2.

Comparing the I–V curves of the bare Mo tip with the same tip with a deposit of one isolated diamond nanoparticle yields a substantial *increase* ($\sim$ 30%) in threshold voltage (Fig. 3, *b* and Table 2). However, after the additional deposition of nanodiamond and the formation of a thicker nanodiamond film, a drastic decrease in threshold voltage ($\sim$ 48%) and an increase in transconductance ($\sim$ 115%) are obvious (Fig. 3, *b* and Table 2).

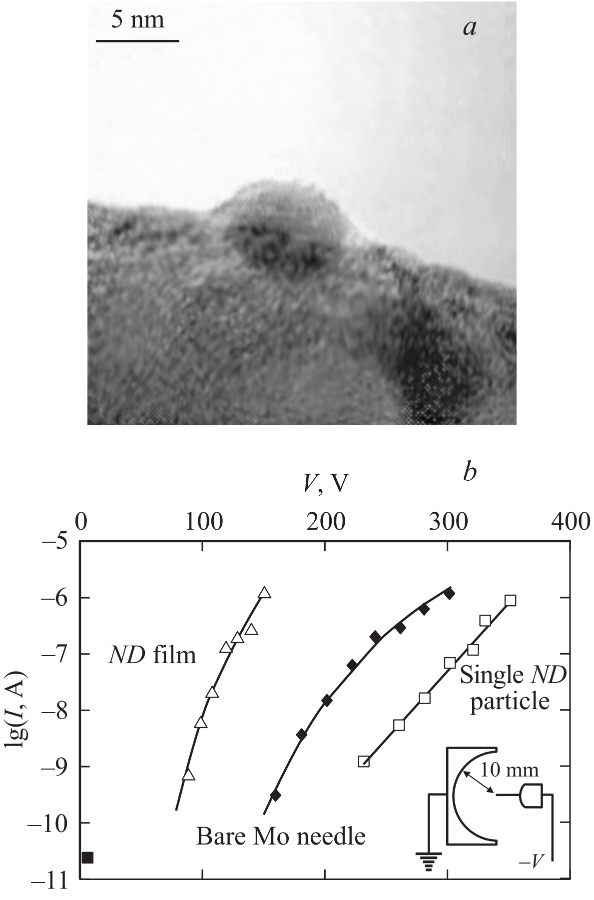

Figure 2. A single, isolated tightly bound, detonation diamond nanodot on the tip of a needle (*a*). Field emission characteristics from the isolated nanodiamond particle shown in Fig. 2, *a* and a nanodiamond film, compared to a bare tip (*b*). Inset: schematic of experimental setup.

4. Simulation of field emission related properties

As part of our efforts to develop a reasonable quantitative model of electron emission from diamond nanoparticles, the electronic structure of diamond nanodots containing between 34 and 1600 carbon atoms was calculated using a self-consisting tight-binding Hamilonian [6,7]. Analysis of these results indicate that for cluster sizes larger than approximately 2 nm quantum confinement effects have relatively little effect, and the electrostatic potential distribution is essentially insensitive to cluster size for clusters larger than 1 nm. The calculated electron affinity (EA) of hydrogenated diamond dots with a majority of their surface area corresponding to (111) facets was approximately — 1.4 eV. This result is close to the experimental value of -1.27 eV [8] and the theoretical value of -2.0 eV calculated using first principals density functional theory by Robertson and Rutter [9] for a bulk hydrogenated (111) diamond surface. In the present paper we address the effect of size on EA in more detail.

It had been demonstrated that the electron affinity of diamond depends on the polar groups on the surface [8]. The sign and magnitude of the surface dipole layer induced potential drop due to specific polar groups enhances and uniquely determines the electron affinity (Fig. 3, *a*). Fig. 3, *b* illustrates continuum electron electrostatic potential distributions within a dielectric sphere with two oppositely charged layers on the surface. The distance between charged layers (0.5 Å) and the related charge density (0.145 e per carbon atom) corresponds to the C–H dipole strength on a (111) diamond surface obtained from the tight-binding simulations. The positive potential drop within the particle shifts the electron energy spectrum up, and hence decreases the EA. Switching the polarity of the charged layers results in an increase in the EA.

For qualitative understanding of the possible effect of size on EA, we assume that introducing a curvature to the initially flat dipole layer corresponding to the macroscopic surface will result in a larger separation of the positively charged H centers for the outer layer (Fig. 3, *a*), and therefore inferior conditions for emission. We also assume that the surface area per carbon atom for nanodiamond is similar to that of macroscopic surfaces. Recently, it has been demonstrated that atomic geometrical parameters of hydrogen terminated nanodiamond do not differ appreciably

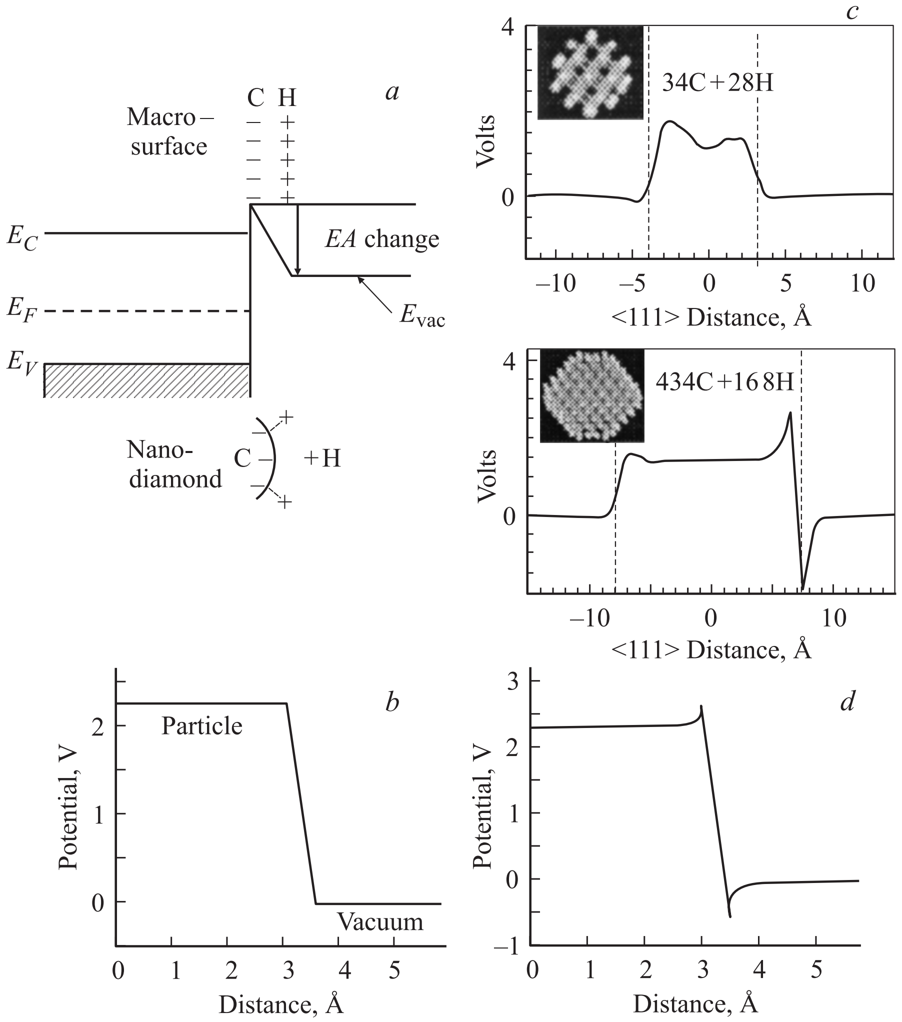

Figure 3. Illustration of size effect of electron affinity properties of nanodiamond particle. Dipole induced negative electron affinity for hydrogenated diamond surface (*a*). Dipoles are shown for macroscopic flat and „curved“ nanoparticle surfaces. Electrostatic potential profile along a radius of a nanodiamond particle calculated for a dielectric sphere with two oppositely charged layers with uniformly distributed charge (*b*) and with pointed charges on the surfaces (*c*). Coulomb potential profile for two diamond clusters calculated with self-consistent tight-binding Hamiltonian (*d*).

from those for bulk diamond [10]. Given the assumptions above the effect of size on the potential drop can be evaluated through the equation for the potential distribution inside a spherical capacitor

$$U = \frac{q \cdot d}{A\varepsilon_a} \frac{R}{R + d}.$$

Here q and d correspond to the charge and length of a dipole, A is surface area per carbon atom ($5.4\,\text{Å}^2$), R is the radius of the inner sphere (carbon atoms), and ε_a is the absolute dielectric permittivity. Fig. 4 illustrates the dependence of the voltage drop on the size of the particle using continuum electrostatic simulations. An appreciable effect takes place only for particles with radii less than ~ 1 nm. Self-consistent tight-binding simulations indicate a less pronounced size effect for the simulated particles having a shape of truncated octahedrons. A slight decrease (~ 0.1 V) of the potential can be seen only for a particle

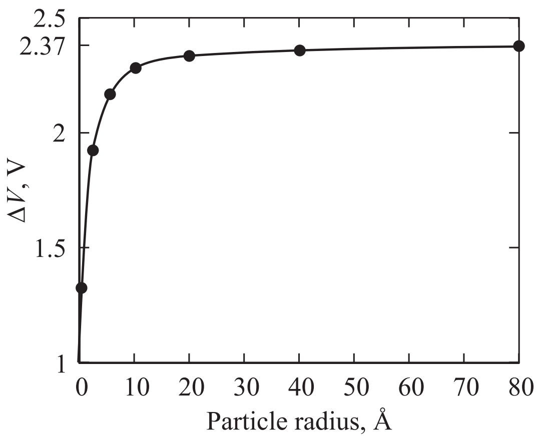

Figure 4. Illustration of the size dependence of the potential drop within a nanodiamond particle, changing the electron affinity. Dipole characteristics are $d = 0.5\,\text{Å}$, $q = 0.14e$; area per carbon atom: $A = 5.4\,\text{Å}^2$.

less than 1 nm in diameter (Fig. 3, *d*). This can be attributed to the fact that simulated particles are faceted and their surfaces are flat rather than spherical as is assumed in the continuum electrostatic calculations above. Therefore based on the present results, the effect of size on the EA of a nanoparticle is sensitive to the shape of the particle.

Finally we point out the presence of small potential spikes in the vicinity of the dipole observed in tight-binding simulations (Fig. 3, *d*). Macroscale descriptions of the negative EA for diamond often neglect these spikes, implying that conduction band electrons experience no barrier to transport into the vacuum. These spikes are associated with particular dipoles. Fig. 3, *c* shows analogous spikes in the potential profile obtained from continuum electrostatic simulations when continuous charge layer distribution interface/boundary conditions on surfaces corresponding to dipole layers are substituted by discrete point charge interface/boundary conditions.

References

[1] V.V. Zhirnov, J.J. Hren. MRS Bulletin **23**, 42 (1998).
[2] V.V. Zhirnov, O.M. Küttel, O. Gröning, A.N. Alimova, P.Y. Detkov, P.I. Belobrov, E. Maillard-Schaller, L. Schlapbach. J. Vac. Sci. Techn. B **17**, 666 (1999).
[3] A.N. Alimova, N.N. Chubun, P.I. Belobrov, P.Y. Detkov, V.V. Zhirnov, J. Vac. Sci. Techn. B **17**, 715 (1999).
[4] T. Tyler, V.V. Zhirnov, A.V. Kvit, D. Kang, J.J. Hren. Appl. Phys. Lett. **82**, 2904 (2003).
[5] S.I. Chukhaeva, L.A. Cheburina. Superhard Materials **2**, 39 (2000).
[6] D.W. Brenner, O.A. Shenderova, D.A. Areshkin, J.D. Schall, S.J. Frankland. Computer Modeling & Eng. Sci. **3**, 643 (2002).
[7] D.A. Areshkin, O.A. Shenderova, J.D. Schall, D.W. Brenner. Mol. Simulat. **29**, 269 (2003).
[8] J. Ristein. Diam. Relat. Mater. **9**, 1129 (2000).
[9] M.J. Rutter, J. Robertson. Phys. Rev. B **57**, 9241 (1998).
[10] S.P. Russo, A.S. Barnard, I.K. Snook. Surf. Rev. Lett. (2004), in press.